Supplementary information

Bionic Nanotheranostic for Multimodal Imaging-Guided NIR-II-Photothermal Cancer Therapy

Meng Zhang[1, 2†], Yuxuan Zhang[1, 3, 4†], Lifeng Hang[2†],Tao Zhang[5], Chuangcai Luo[1, 4], Wuming Li[2], Yiqiang Sun[6], Hua Wen[2], Yiyu Chen[2], Guihua Jiang[1, 2*] and Xiaofen Ma[2*]

[1] The Second School of Clinical Medicine, Southern Medical University, Guangzhou 510282, China.

[2] The Department of Medical Imaging, Guangzhou Key Laboratory of Molecular Functional Imaging and Artificial Intelligence for Major Brain Diseases, Guangdong Second Provincial General Hospital, Guangzhou 510317, China

[3] Department of Neurosurgery, Institute of Neuroscience, The Second Affiliated Hospital of Guangzhou Medical University, Guangzhou, 510260, China.

[4] The National Key Clinical Specialty, Department of Neurosurgery, Zhujiang Hospital, Southern Medical University, Guangzhou 510282, China.

[5] School of Physical and Mathematical Sciences, Nanyang Technological University, 21 Nanyang Link, Singapore 637371, Singapore.

[6] School of Chemistry and Chemical Engineering, University of Jinan, Jinan 250022, China

[†] Contributed equally

* Corresponding author

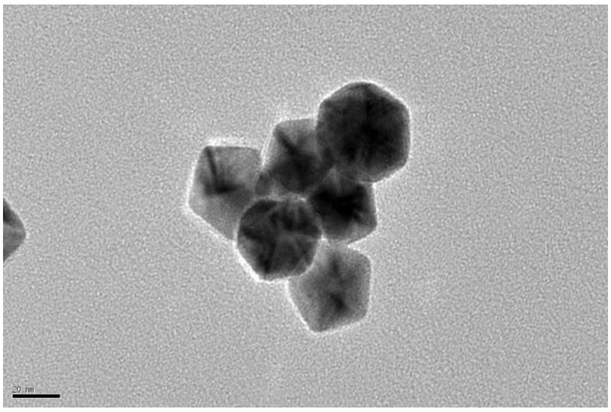

Fig. S1. TEM image of gold decahedron (scale bar: 20 nm).

Fig. S2. TEM image of Au NBP (scale bar: 500 nm).

Fig. S3. TEM image of Au@MnO_2 (scale bar: 50 nm).

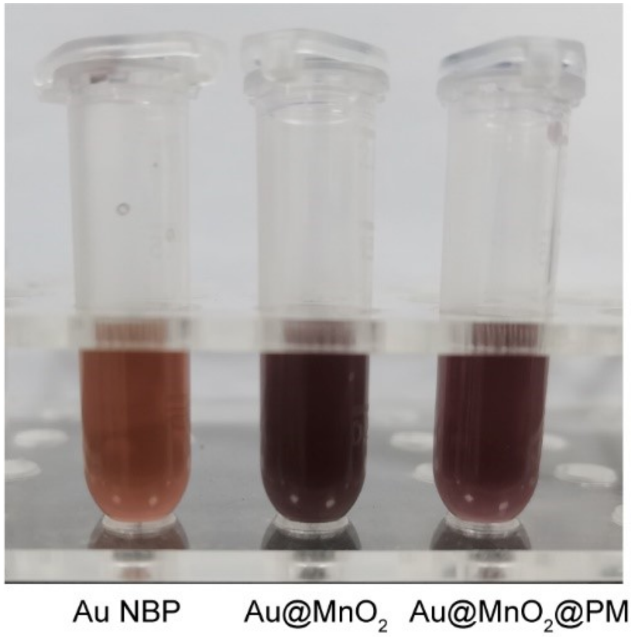

Fig. S4. Digital image of Au NBP (left), Au@MnO_2 (middle) and Au@MnO_2@PM (right).

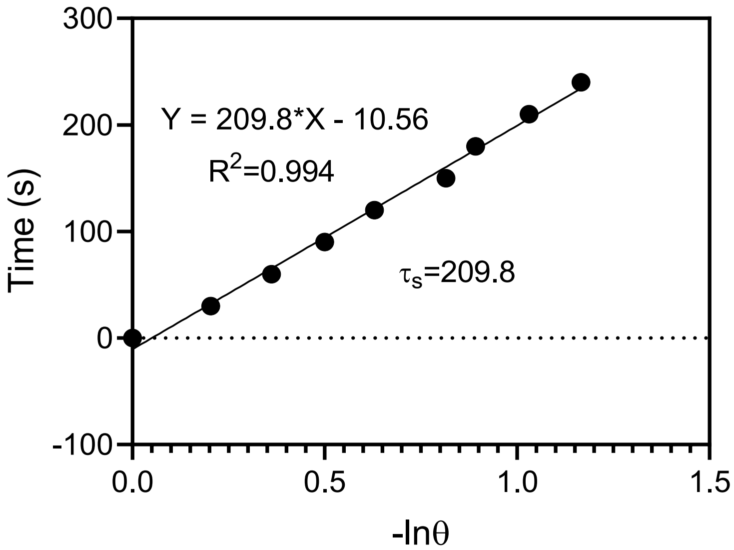

Fig. S5. Calculation of photothermal conversion efficiency (η) of AMP.

Calculation of the Photothermal Conversion Efficiency.

Following Roper's report (J. Phys. Chem. C 2007, 111, 3636), the total energy balance for the system can be expressed by Eq. 1:

$$\Sigma_i m_i C_{p,i}\frac{dT}{dt} = Q_{NC} + Q_{Dis} - Q_{surr} \quad (1)$$

Where m and C_p are the mass and heat capacity of water, respectively, T is the solution temperature, Q_{NC} is the energy inputted by NCs, Q_{Dis} is the baseline energy inputted by the sample cell, and Q_{surr} is heat conduction away from the system surface by air.

The laser-induced source term, represents heat dissipated by electron-phonon relaxation of the plasmons on the AMP surface under the irradiation of 1064 nm laser:

$$Q_{NC} = I(1 - A^{-1064})\eta \quad (2)$$

Where I is incident laser power, η is the conversion efficiency from incident laser energy to thermal energy, and A_{1064} is the absorbance of the AMP at wavelength of 1064 nm. In addition, source term, Q_{Dis}, expresses heat dissipated from light absorbed by the quartz sample cell itself, and it was measured independently to be 113.75 mW using a quartz cuvette cell containing pure water without any AMP. Q_{surr} is linear with temperature for the outgoing thermal energy, as given by Eq. 3

$$Q_{surr} = hS(T - T_{surr}) \quad (3)$$

Where h is heat transfer coefficient, S is the surface area of the container, and T_{Surr} is ambient temperature of the surroundings.

Once the laser power is defined, the heat input (Q_{NC} + Q_{Dis}) will be finite. Since the heat output (Q_{Surr}) is increased along with the increase of the temperature according to the Eq. 3, the system temperature will rise to a maximum when the heat input is equal to heat output:

$$Q_{NC} + Q_{Dis} = Q_{surr-max} = hS(T_{max} - T_{surr}) \quad (4)$$

Where the $Q_{surr\text{-}max}$ is heat conduction away from the system surface by air when the sample cell reaches the equilibrium temperature, and T_{max} is the equilibrium temperature. The 1064 nm laser heat conversion efficiency (η) can be determined by substituting Eq. 2 for Q_{NC} into Eq. 4 and rearranging to get

$$\eta = \frac{hS(T_{max} - T_{surr}) - Q_{Dis}}{I(1 - 10^{-A_{1064}})} \quad (5)$$

Where Q_{Dis} was measured independently to be 113.75 mW, the (T_{max}-T_{Surr}) was 24.4 °C according to Figure 1G and 1H, I is 785 mW, A_{1064} is the absorbance (1) of AMP at 1064 nm (Figure 1F). Thus, only the hS remains unknown for calculating η.

In order to get the hS, a dimensionless driving force temperature, θ is introduced using the maximum system temperature, T_{max}

$$\theta = \frac{T - T_{surr}}{T_{max} - T_{surr}} \quad (6)$$

and a sample system time constant τ_s,

$$\tau_s = \frac{\Sigma_i m_i C_{p,i}}{hS} \quad (7)$$

which is substituted into Eq. 1 and rearranged to yield

$$\frac{d\theta}{dt} = \frac{1}{\tau_s}[\frac{Q_{NC} + Q_{Dis}}{hS(T_{max} - T_{surr})} - \theta] \quad (8)$$

At the cooling stage of the aqueous dispersion of the AMP, the light source was shut off, the Q_{NC} +Q_{Dis} = 0, reducing the Eq. 9

$$dt = -\tau_s \frac{d\theta}{\theta} \quad (9)$$

and integrating, giving the expression

$$\tau = -\tau_s ln\theta \quad (10)$$

finally, find the value of photothermal conversion efficiency (η)

$$\eta = \frac{hS(T_{max} - T_{surr}) - Q_{Dis}}{I(1 - 10^{-A_{1064}})} = \frac{(20.16 \times 24.4\,mW - 113.7\,mW)}{(785mW \times (1 - 10^{-1.0804})} = 52.07\%$$

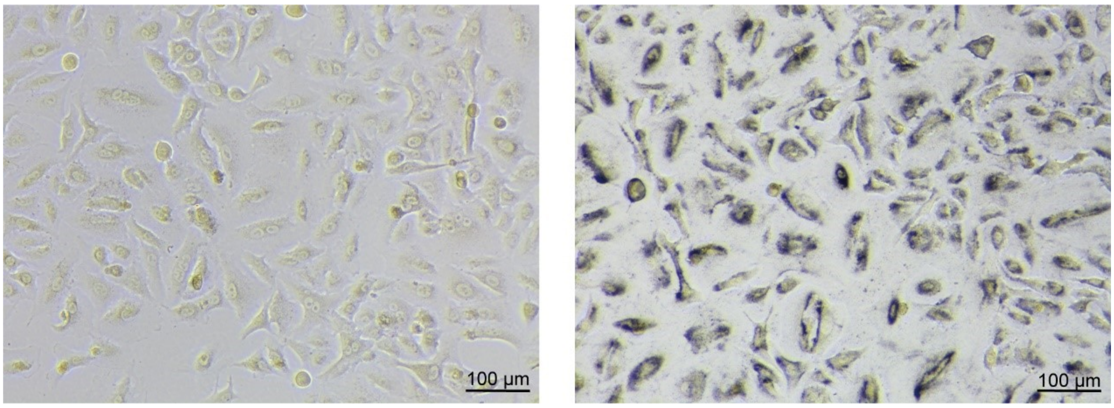

Fig. S6. Optical microscopy images were taken 24 hours after the addition of PBS (left) and AMP (right) to A549 cell culture medium. Scale bar: 100 μm

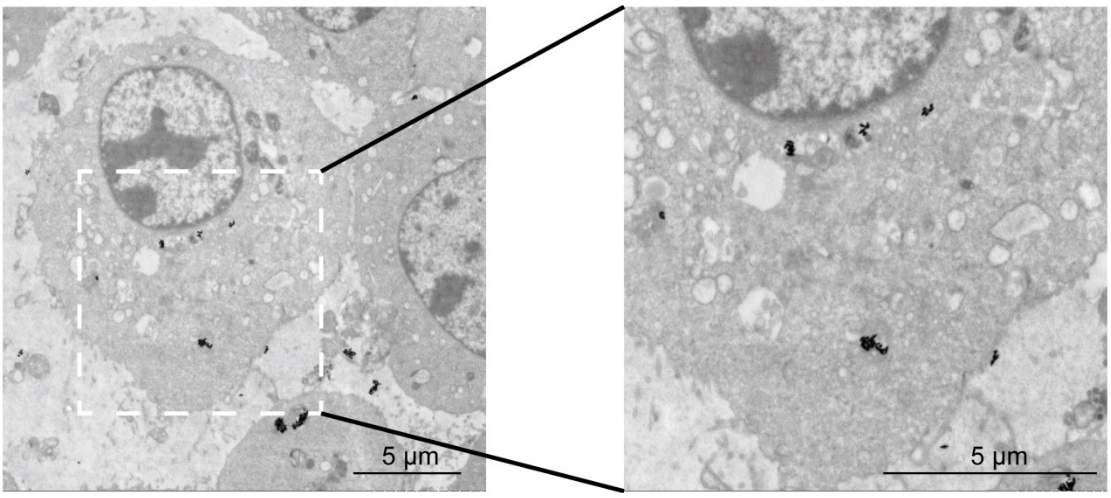

Fig. S7. Low magnification (left) and high magnification (right) images of AMP uptake by A549 cells obtained by transmission electron microscopy. Scale bar: 5 μm.

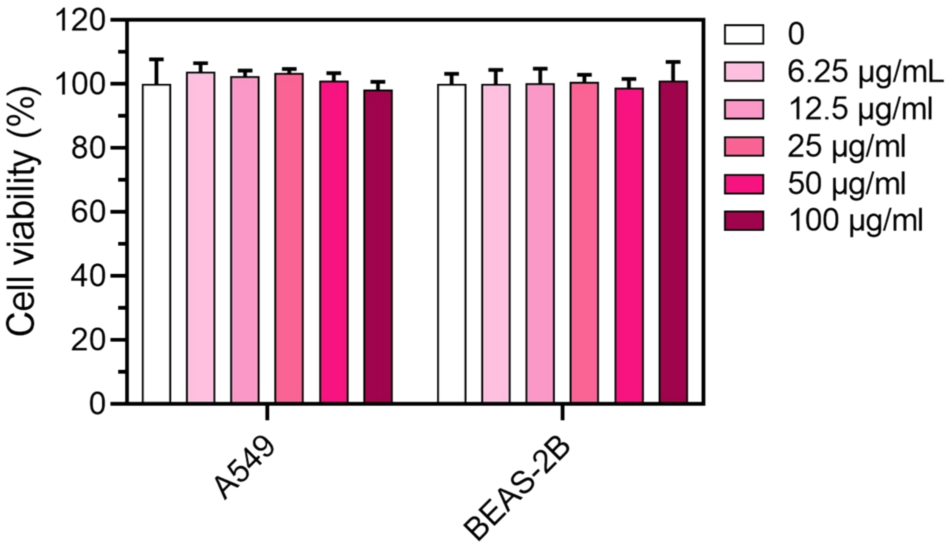

Fig. S8. Cell viability of A549 cells and BEAS-2B cells after co-incubation with various concentrations of AMP for 48 h.

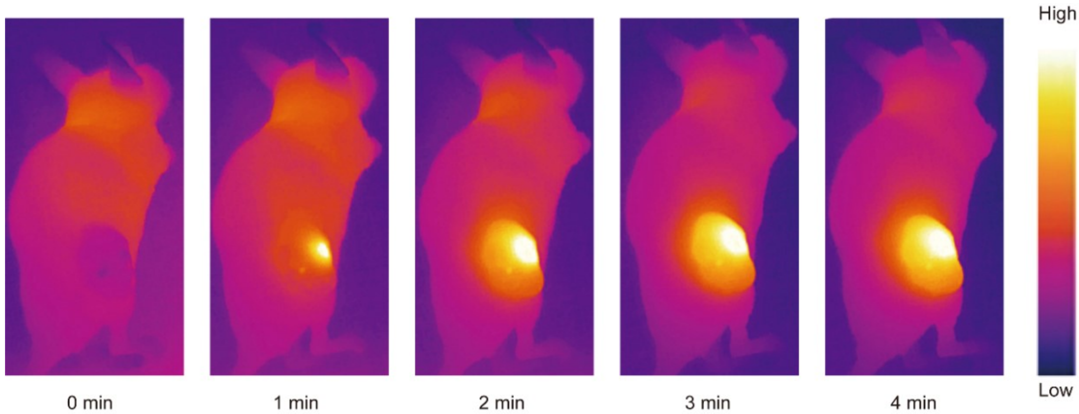

Fig. S9. Corresponding infrared thermal images (1064 nm laser doses: 1.0 W cm^{-2})

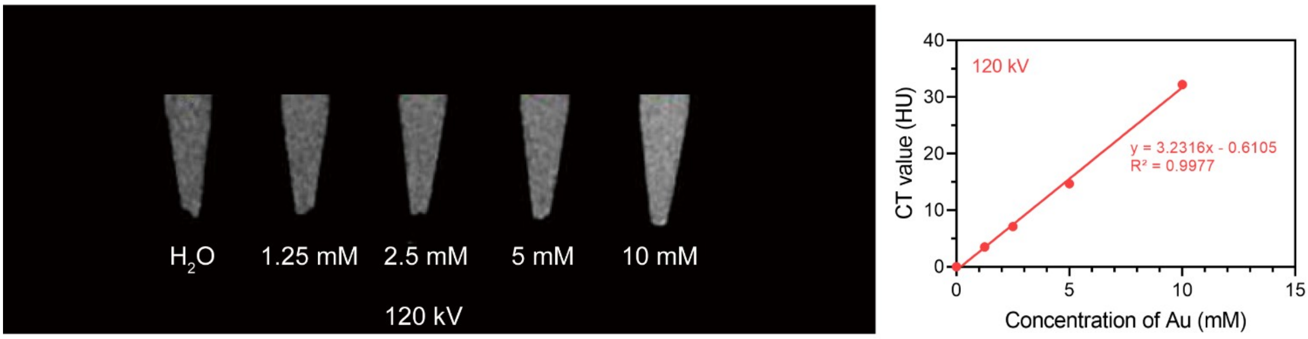

Fig. S10. CT images of different concentrations of AMP at 120kV (left) and corresponding CT value (right).

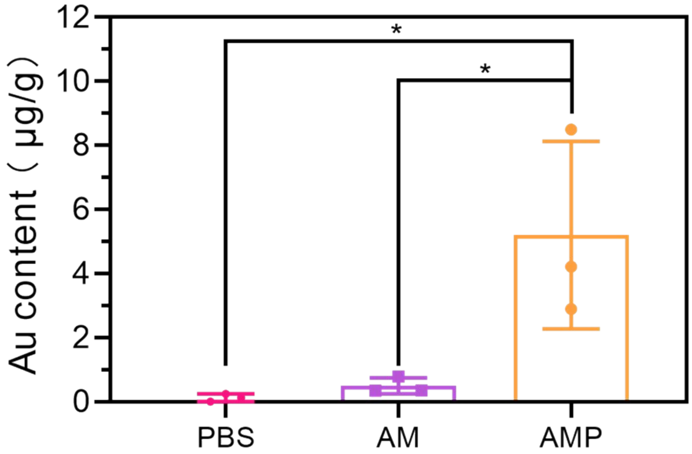

Fig. S11. The bioaccumulation of Au in tumor tissue in PBS ,AM and AMP groups. *$P < 0.05$.

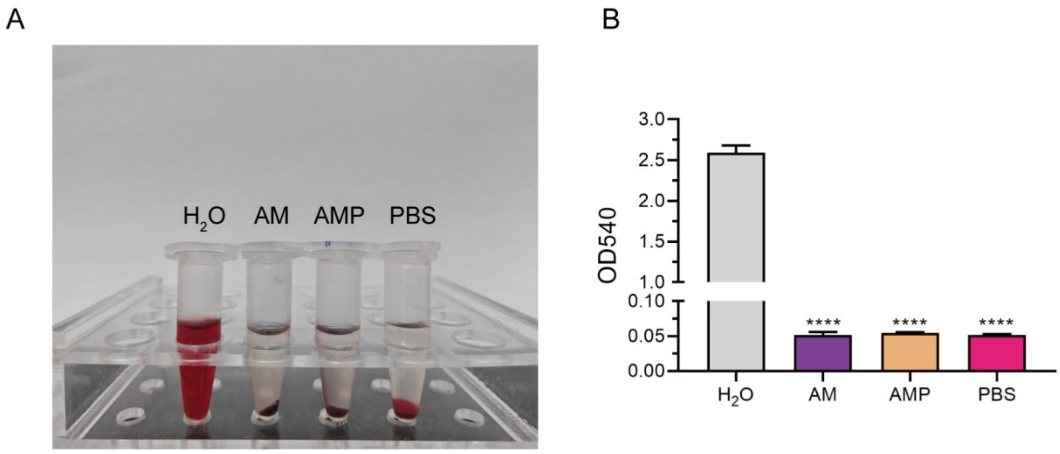

Fig. S12. (A) Photograph of the RBC solution incubated with 100ug mL^{-1} of AM or AMP. The H_2O group and PBS group were used as positive and negative control group, respectively. (B) Absorbance at 540 nm of the supernatants of different groups solution. ****$P < 0.0001$.

Table S1. Photothermal performance of recently reported photothermal agents employed in NIR-II window.

Photothermal agents	PTCE	Photothermal agents	PTCE
AMPs (this work)	0.520	Ti_3C_2/CA_4@PLEL nanohydrogel[1]	0.414
Au/Ag NRs[2]	0.288	Au-Au nanocoral[3]	0.672
Au NPL@TiO_2[4]	0.420	anti-STR-CO-GNSs[5]	0.319
Au@MOF-DOX[6]	0.302	PLNP-Bi_2S_3[7]	0.44
Au NSs[8]	0.130	TA-Si-Au[9]	0.241

PTCE, photothermal conversion efficiency.

1 Tao, N. *et al.* Minimally Invasive Antitumor Therapy Using Biodegradable Nanocomposite Micellar Hydrogel with Functionalities of NIR-II Photothermal Ablation and Vascular Disruption. *ACS Appl Bio Mater* **3**, 4531-4542, doi:10.1021/acsabm.0c00465 (2020).

2 Mei, Z. *et al.* Activatable NIR-II photoacoustic imaging and photochemical synergistic therapy of MRSA infections using miniature Au/Ag nanorods. *Biomaterials* **251**, 120092, doi:10.1016/j.biomaterials.2020.120092 (2020).

3 Jia, J. *et al.* Fine‐Tuning the Homometallic Interface of Au‐on‐Au Nanorods and Their Photothermal Therapy in the NIR‐II Window. *Angewandte Chemie International Edition* **59**, 14443-14448, doi:10.1002/anie.202000474 (2020).

4 Gao, F. *et al.* Titania-coated 2D gold nanoplates as nanoagents for synergistic photothermal/sonodynamic therapy in the second near-infrared window. *Nanoscale* **11**, 2374-2384, doi:10.1039/c8nr07188h (2019).

5 Manivasagan, P. *et al.* Antibody-conjugated and streptomycin-chitosan oligosaccharide-modified gold nanoshells for synergistic chemo-photothermal therapy of drug-resistant bacterial infection. *J Adv Res* **48**, 87-104, doi:10.1016/j.jare.2022.08.009 (2023).

6 Deng, X. *et al.* Yolk–Shell Structured Au Nanostar@Metal–Organic Framework for Synergistic Chemo-photothermal Therapy in the Second Near-Infrared Window. *Nano Letters* **19**, 6772-6780, doi:10.1021/acs.nanolett.9b01716 (2019).

7 Meng, Y. *et al.* Photothermal conversion performance and acid-induced aggregation of PLNP-Bi(2)S(3) composite nanoplatforms. *Dalton Trans* **51**, 5285-5295, doi:10.1039/d1dt04215g (2022).

8 Song, C. *et al.* Gold nanostars for cancer cell-targeted SERS-imaging and NIR light-triggered plasmonic photothermal therapy (PPTT) in the first and second biological windows. *Journal of Materials Chemistry B* **7**, 2001-2008, doi:10.1039/c9tb00061e (2019).

9 Sun, L. N. *et al.* Silicon nanowires decorated with gold nanoparticles via in situ reduction for photoacoustic imaging-guided photothermal cancer therapy. *Journal of Materials Chemistry B* **7**, 4393-4401, doi:10.1039/c9tb00147f (2019).